

# Fusion – Fission Hybrid System With Molten Salt Blanket for Nuclear Waste Transmutation\*

**R. Plukiene, D. Ridikas**<sup>†</sup> for the Mini-Inca collaboration

CEA Saclay, DSM/DAPNIA/SPhN, F-91191 Gif-sur-Yvette Cedex, France

**E.T. Cheng**

TSI Research Inc., P.O. Box 2754, Rancho Santa Fe, California 92067 U.S.A.

## Abstract

An intensive neutron source is needed for the transmutation process of nuclear waste. A plasma based fusion device is naturally a candidate neutron source. In this paper we analyze a typical molten salt (flibe) blanket, driven by a plasma based fusion device, dedicated to burn actinides extracted from the LWR spent fuel. Performance parameters such as  $k_{scr}$ , burnup, fluxes and equilibrium conditions were obtained to assess the characteristics of a flibe based transmutation plant. It seems that nearly 1.1 metric tons of spent fuel TRU could be burned annually with an output of 3 GW<sub>th</sub> fission power. Detailed burnup calculations show that equilibrium conditions of the fuel concentration in the flibe transmutation blanket could be achieved, provided that fission products were removed at least in part and fresh spent fuel TRU was added during burnup on-line.

---

\*Proceedings of the XIXth Int. Autumn School on New Perspectives with Nuclear Radioactivity (NRAD2001), 8-13 October 2001, Lisbon, Portugal

<sup>†</sup>E-mail: ridikas@cea.fr

# 1 Introduction

The main goal of this work is to investigate the performance of the dedicated molten salt (flibe) blanket for nuclear waste transmutation as a function of different treatment of fission products as well as different refueling of already destroyed actinides. This work is a continuation of the related studies on a flibe based actinide transmutation hybrid system driven by a fusion device [1, 2, 3]. Below we will present only a brief summary of the concept sufficient for understanding this follow-up study. A detailed description of the fusion-fission hybrid system including some burnup calculations can be found in Refs. [1, 2].

In order to transmute efficiently the nuclear waste, a high intensity neutron source is needed. It seems that an inertial confinement fusion (ICF) device could provide with a neutron source as intense as a high power accelerator, i.e. of the order of  $10^{18} - 10^{19}$  n/s. A molten salt (LiF-BeF<sub>2</sub>-(TRU)F<sub>4</sub>) blanket, surrounding this neutron source, then serves as a medium for transuranic actinides (TRU) to be burned. Flibe also has a function of both coolant and carrier of tritium breeding material (<sup>6</sup>Li in this case). A well known advantage of the molten salt is a possibility of both refueling of burned TRU and extraction of fission products (FP) on-line. Namely these two parameters we are going to investigate in more detail in this work.

The main characteristics of the fusion-fission hybrid system are presented in Table 1 [1]. In order to produce 3000 MW<sub>th</sub> fission power, ~200 MW power fusion device is sufficient to

fusion power	200MW
fission power	3000MW <sub>th</sub>
k <sub>eff</sub> at equilibrium	0.743
M <sub>E</sub> at equilibrium	19
TBR at equilibrium	1.4
Initial TRU composition	LWR spent fuel
Initial TRU inventory (kg)	3045

Table 1: Characteristics of fusion based fission blanket [1]. M<sub>E</sub> stands for the energy multiplication of the system, while TBR for the tritium breeding ratio.

provide with an external neutron source of the order of  $\sim 8 \times 10^{19}$  n/s. A simplified fusion-fission hybrid system was modelled with the main geometry and material parameters given in Table 2. Fig. 1 presents a detailed geometry setup used in our calculations. Flibe(a) contained 0.1% of <sup>6</sup>Li in lithium. Flibe(b) density was  $8.5156 \times 10^{22}$  atoms/cm<sup>3</sup> (2g/cm<sup>3</sup>) and TRU material density in flibe(b) was  $1.87 \times 10^{20}$  atoms/cm<sup>3</sup> (0.0074g/cm<sup>3</sup> of flibe) or 0.5 molar % in flibe. 0.6% <sup>6</sup>Li enrichment for flibe(b) was taken as a reference case [1]. In both cases <sup>6</sup>Li in lithium served as a breeding material for tritium production. The initial loading and subsequent feeding TRU compositions were those from the LWR spent fuel when fission products and uranium are separated (to be provided in detail later in this paper in Fig. 8).

## 2 Modelling tools and procedure

All calculations on flibe based actinide transmutation blanket were made employing Monteburns code system [4] - an automatic-cyclic coupling of the MCNP [5] and ORIGEN2 [6] codes. Monteburns was already successfully benchmarked by simulating the uranium based fuel cycle of the high flux reactor at ILL Grenoble [7] and GT-MHR (Gas Turbine - Modular Helium cooled Reactor) in the case of plutonium (uranium free) fuel cycle [8]. In our case MCNP was used to

Zone name	Radius (cm) $R_i-R_{i+1}$	Thickness (cm)	Material composition
Cavity	0-200	200	void
Liquid wall	200-201	1	flibe(a)
Metallic wall	201-201.3	0.3	SS316; 50%
Graphite	201.3-202.3	1	graphite
Blanket			
Region 1	202.3-217.3	15	flibe(b)
Region 2	217.3-232.3	15	flibe(b)
Region 3	232.3-247.3	15	flibe(b)
Region 4	247.3-262.3	15	flibe(b)
Reflector	262.3-282.3	20	graphite
Envelope	282.3-287.5	5	SS316; 50%

Table 2: Neutronics model: zone dimension and material compositions for a molten salt transmutation blanket as from [1]. Also see Fig. 1

obtain  $k_{eff}$  in the mode of a criticality eigenvalue problem (*kcode* card in MCNP input), and also to estimate neutron flux as well as  $k_{src}$  in its external source mode (*sdef* card in the MCNP input). In this case  $k_{src}$  is defined as:

$$k_{src} = (M_n - 1)/(M_n - 1/\nu), \quad (1)$$

where  $\nu$  is an average number of neutrons per fission and  $M_n$  is a total neutron multiplication factor of the system. We note separately that all burnup calculations were done employing this external source mode.

The advantage of the MonteBurns code is that it can use different nuclear data libraries as long as they are compatible with MCNP format (see for example Ref. [9]). For all structure materials and actinides we have chosen ENDF data files [10] being most frequently employed, while for fission products JENDL data library [11] was taken due to the biggest number of fission products available ( $\sim 200$ ).

The main goal of the modelling was to find the equilibrium conditions of the fusion-fission hybrid system and to investigate how these conditions could be influenced due to the different modes of refueling (continuous or discrete feeding) and also due to the different treatment of fission products (partial/full and/or continuous/discrete removal). For that purpose we had to:

- stabilize an effective neutron multiplication coefficient and the total TRU mass in the system,
- define the actual amount of fresh TRU material ( $\Delta M_{TRU}$ ) to be fueled on-line,
- try to keep the neutron spectrum  $\Phi_n(E)$  constant as a function of burnup.

In all cases the fission power was kept constant ( $3000\text{MW}_{th}$ ), what corresponds to a variable fusion power of the fusion device (see Fig. 7 in the coming Section). In our simulations this simply implies a renormalization of the absolute neutron flux when an effective neutron multiplication coefficient of the system is changed.

## 3 Results

### 3.1 Neutron Flux and Energy Spectra

Table 3 presents the main neutron flux characteristics in different regions of the molten salt

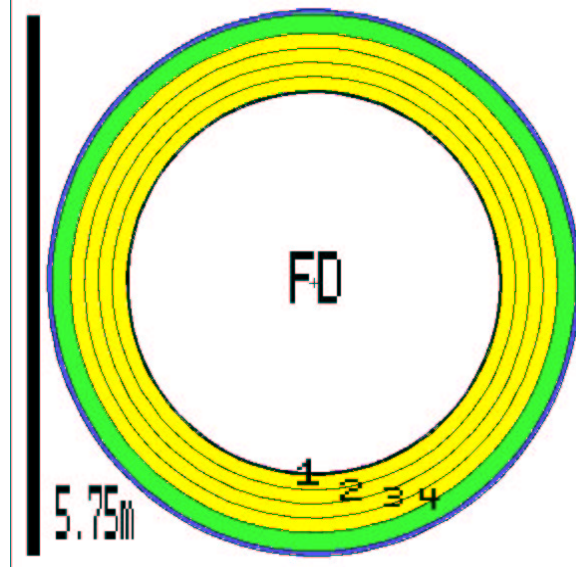


Figure 1: A simplified geometry of the fusion-fission hybrid system used in the calculations. FD stands for "fusion device". See text and Table 1 for details.

Zone name	$\phi_n(\text{total})$ (n/s cm <sup>2</sup> )	$\phi_n(E_n > 0.1\text{MeV})$ (%)
Region 1	$2.47 \times 10^{15}$	26.2
Region 2	$1.84 \times 10^{15}$	22.4
Region 3	$1.22 \times 10^{15}$	20.4
Region 4	$0.75 \times 10^{15}$	20.6
Regions 1-4	$1.48 \times 10^{15}$	22.9

Table 3: Neutron flux characteristics in different regions of the molten salt transmutation blanket at the beginning of the irradiation. Also see Table 1.

transmutation blanket (see Fig. 1). Corresponding energy spectra are presented in Fig. 2.

We note separately that the averaged neutron flux is very high and corresponds to the flux typical only for high flux reactors, and the fast neutron flux ( $E > 0.1$  MeV) is about  $10^{22}$  n/cm<sup>2</sup> per full power year. In addition, the amount of thermal neutrons is very small (<1%). Most of the neutrons are epithermal or fast, what could favor the transmutation of actinides in the resonance region.

Fig. 3 gives a variation of averaged neutron spectrum as a function of burnup. It is clearly seen that the neutron spectrum remains stable. In addition, this is also true if either continuous or discrete feeding of a fresh fuel is simulated. This might justify a less time consuming approach for the fuel burnup, i.e. as a good approximation one could calculate the neutron flux (and consequently flux weighted neutron cross sections) only once and perform burnup calculations with a constant neutron spectrum.

Finally, Fig. 4 gives one group flux weighted neutron capture and fission cross sections to be compared to other transmutation systems being either critical or accelerator driven.

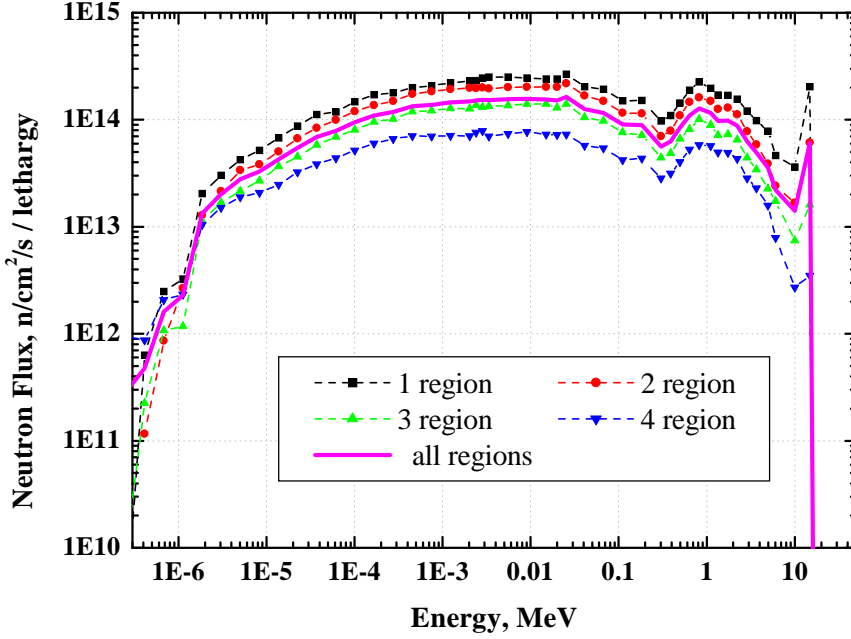


Figure 2: Profile of the neutron spectrum in different fibe regions. A solid line indicates the average neutron flux over all regions.

### 3.2 Equilibrium conditions

A typical evolution of the TRU isotopic composition is presented in Fig. 5. This is the case when the system is refueled continuously. In addition, the fission products are also continuously removed on-line at 100% rate.

In order to define the equilibrium we employ the following arbitrary procedure. Since not all actinides are stabilized even after 2000 days of operation (Cm isotopes in particular), we assume that the system reaches equilibrium when the variation of the mass of each Pu isotope is less than, say, 4% with respect to the actual plutonium mass in the blanket. This is represented in detail in Fig. 6, where the variational dependence of Pu isotope masses during the irradiation is illustrated. According to this analysis we conclude that the equilibrium is reached after about  $1000 \pm 50$  days of irradiation.

A corresponding behavior of  $k_{scr}$  and required fusion power  $P_{fusion}$  at the constant fission power of  $3000 \text{ MW}_{th}$  are presented in Fig. 7. The excursion of  $k_{scr}$  occurs mainly due to the conversion of  $^{240}\text{Pu}$  into  $^{241}\text{Pu}$  during the early stage of irradiation (see Figs. 5 and 6 for detailed mass dependence of  $^{241}\text{Pu}$  during irradiation). The values of  $k_{scr}$  were calculated in the case when all fission products are continuously removed from the blanket. We remind that 1 MW fusion power corresponds to the external neutron source intensity of  $\sim 4 \times 10^{17}$  n/s of 14 MeV neutrons.

Finally we note that  $\sim 3.1$  kg of TRU is burned per day when the equilibrium situation is reached, what corresponds to nearly 1.1 metric tons of TRU burned annually. Fig. 8 gives detailed isotopic composition of the initial TRU vector and also at equilibrium, i.e. after 1000 days of irradiation. Different options DD, DC, CD, and CC correspond to different refueling conditions and also to different treatment of the fission products (see the caption of Fig 8). For comparison we also present the results reported in Ref. [1]. We note that in all cases equilib-

Time, days	$\Phi_n$ , % (Discrete)					$\Phi_n$ , % (Continuous)				
	[0.,1.] eV	[1.,100.] eV	[.1,100.] keV	[.1,1.] MeV	[1.,20] MeV	[0.,1.] eV	[1.,100.] eV	[.1,100.] keV	[.1,1.] MeV	[1.,20] MeV
0	0.16	14.58	62.49	12.28	10.45	0.04	14.58	62.49	12.28	10.45
400	0.16	15.37	62.07	12.02	10.33	0.03	14.84	62.55	12.24	10.19
800	0.16	15.52	61.87	12.07	10.35	0.04	15.09	62.33	12.18	10.22
1200	0.14	15.43	61.87	12.11	10.42	0.04	15.12	62.12	12.2	10.38
1600	0.15	15.30	61.98	12.03	10.51	0.04	15.25	62.03	12.08	10.47
2000	0.16	15.33	61.72	12.14	10.62	0.03	14.93	62.22	12.22	10.47

Figure 3: Averaged neutron spectrum over all fiibe regions, presented in different energy groups (%) as a function of burnup.

	$\sigma_c$ , b	$\sigma_f$ , b	$\sigma_f/\sigma_c$
<sup>237</sup> Np	18.20	0.26	0.01
<sup>238</sup> Pu	6.79	1.90	0.28
<sup>239</sup> Pu	7.70	10.80	1.40
<sup>240</sup> Pu	14.60	0.31	0.02
<sup>241</sup> Pu	6.48	20.70	3.20
<sup>242</sup> Pu	14.20	0.22	0.02
<sup>243</sup> Pu	5.93	9.54	1.61
<sup>241</sup> Am	20.60	0.36	0.02
<sup>242*</sup> Am	7.20	44.00	6.10
<sup>243</sup> Am	27.50	0.21	0.01
<sup>243</sup> Cm	3.25	21.10	6.49
<sup>244</sup> Cm	16.30	0.65	0.04
<sup>245</sup> Cm	3.25	22.70	7.00
<sup>246</sup> Cm	4.93	0.31	0.06

Figure 4: One group flux weighted neutron capture and fission cross sections and corresponding ratio for a number of selected actinides.

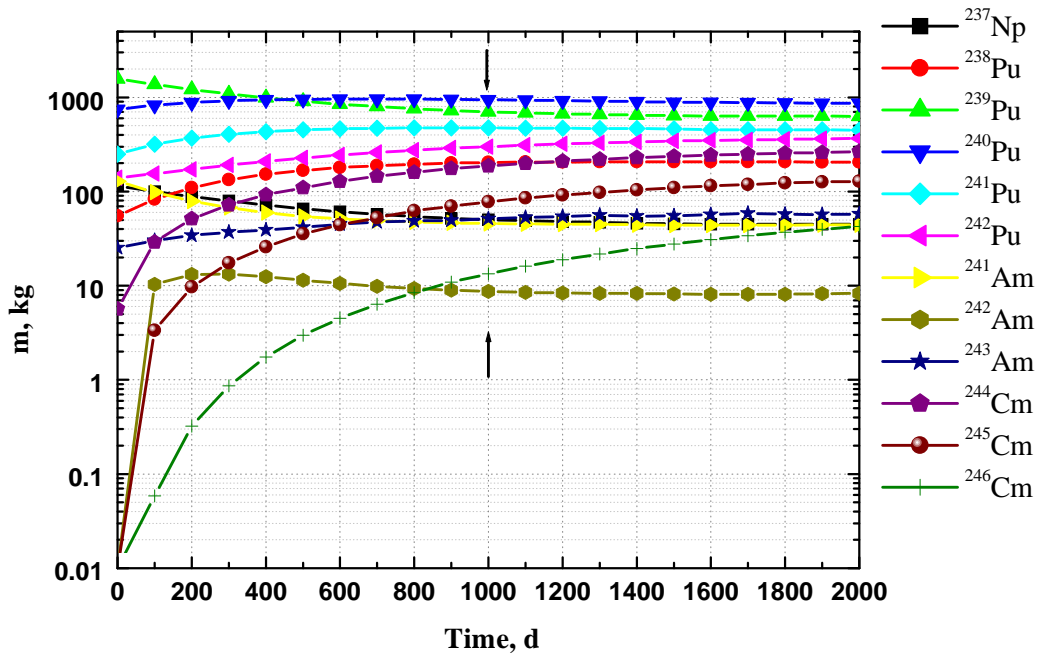


Figure 5: TRU mass dependence on irradiation time: continuous feeding with 3.1 kg/d of TRU and continuous removal of all fission products.

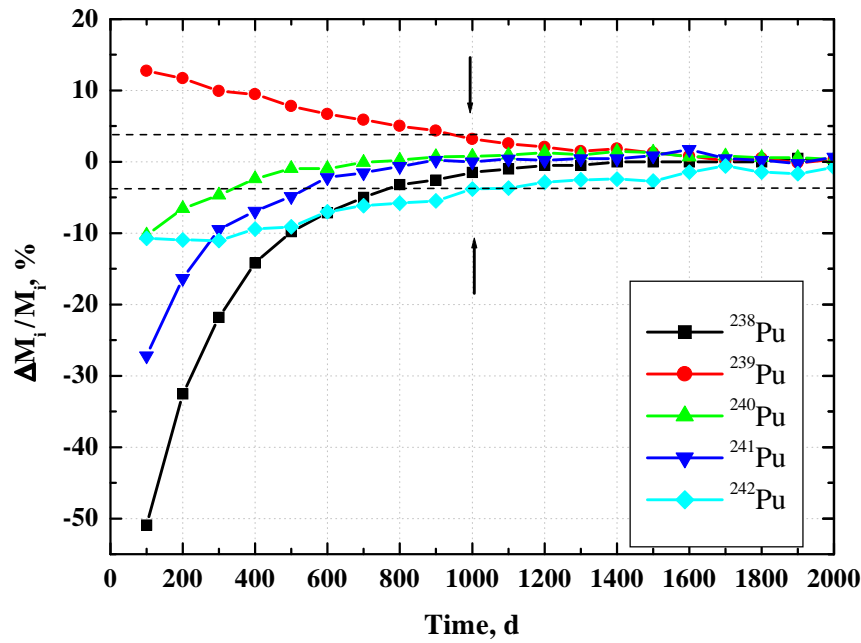


Figure 6: Variation in mass (%) of Pu isotopes as a function of the irradiation time in the case of continuous feeding of TRU material and total removal of FP.  $i$  stands for a different isotope of Pu.

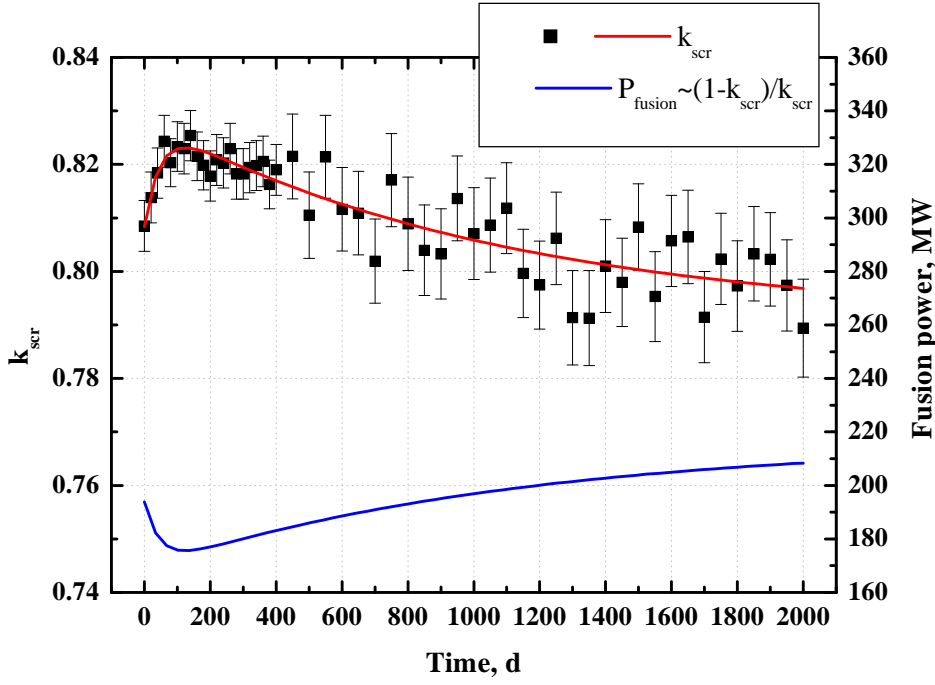


Figure 7: A behavior of  $k_{scr} \pm 1\sigma$  and required fusion power (or external neutron source intensity)  $P_{fusion}$  as a function of irradiation. The constant fission power of  $3000 \text{ MW}_{th}$  was kept.

Stage	Initial	Equilibrium				Ref.[1]
Cases		DD	DC	CD	CC	
Time, days	0	1000	1000	1000	1000	~980
$^{237}\text{Np}$ , %	3.78	1.50	1.48	1.63	1.62	1.51
<b>Total Np, %</b>	<b>3.78</b>	<b>1.51</b>	<b>1.50</b>	<b>1.64</b>	<b>1.64</b>	<b>0.00</b>
$^{238}\text{Pu}$ , %	1.81	6.92	6.98	6.47	6.57	4.83
$^{239}\text{Pu}$ , %	51.64	21.23	21.05	22.95	22.75	20.90
$^{240}\text{Pu}$ , %	24.61	29.49	29.16	30.42	30.58	30.10
$^{241}\text{Pu}$ , %	8.22	16.09	16.18	15.35	15.31	15.70
$^{242}\text{Pu}$ , %	4.61	10.14	9.96	9.90	9.71	10.70
<b>Total Pu, %</b>	<b>90.89</b>	<b>83.87</b>	<b>83.33</b>	<b>85.09</b>	<b>84.92</b>	<b>82.23</b>
$^{241}\text{Am}$ , %	4.21	1.34	1.32	1.49	1.48	1.49
$^{242m}\text{Am}$ , %	0	0.29	0.28	0.29	0.28	0.60
$^{243}\text{Am}$ , %	0.83	1.82	1.88	1.60	1.67	4.80
<b>Total Am, %</b>	<b>5.04</b>	<b>3.45</b>	<b>3.48</b>	<b>3.38</b>	<b>3.43</b>	<b>6.89</b>
$^{244}\text{Cm}$ , %	0.19	6.74	6.87	5.83	6.05	6.31
$^{245}\text{Cm}$ , %	0	2.91	2.99	2.45	2.52	2.68
$^{246}\text{Cm}$ , %	0	0.52	0.54	0.41	0.43	0.50
<b>Total Cm, %</b>	<b>0.19</b>	<b>10.17</b>	<b>10.40</b>	<b>8.69</b>	<b>9.00</b>	<b>9.49</b>
<b>Others, %</b>		<b>1.01</b>	<b>1.31</b>	<b>1.21</b>	<b>1.03</b>	

Figure 8: TRU composition (%) in the molten salt at initial and equilibrium stages: DD – discrete feeding and discrete FP removal; DC – discrete feeding and continuous FP removal; CD – continuous feeding and discrete FP removal; DD – continuous feeding and continuous FP removal; in all cases 100% of fission products were removed.



rium is reached and a reasonable agreement between Pu, Np and Cm isotopes is obtained when compared to the calculations reported in Ref. [1]. On the other hand, in our case we obtained much less  $^{242}\text{Am}$  and  $^{243}\text{Am}$ . This difference might be due to the different data libraries used and still has to be studied in detail.

### 3.3 Effect of different feeding options

In general it is preferred that an effective neutron multiplication factor is as stable as possible for any nuclear reactor being either critical or sub-critical. Fig. 9 illustrates the effect of different feeding options on  $k_{scr}$ . As one could expect, a discrete feeding results in sharp variation of

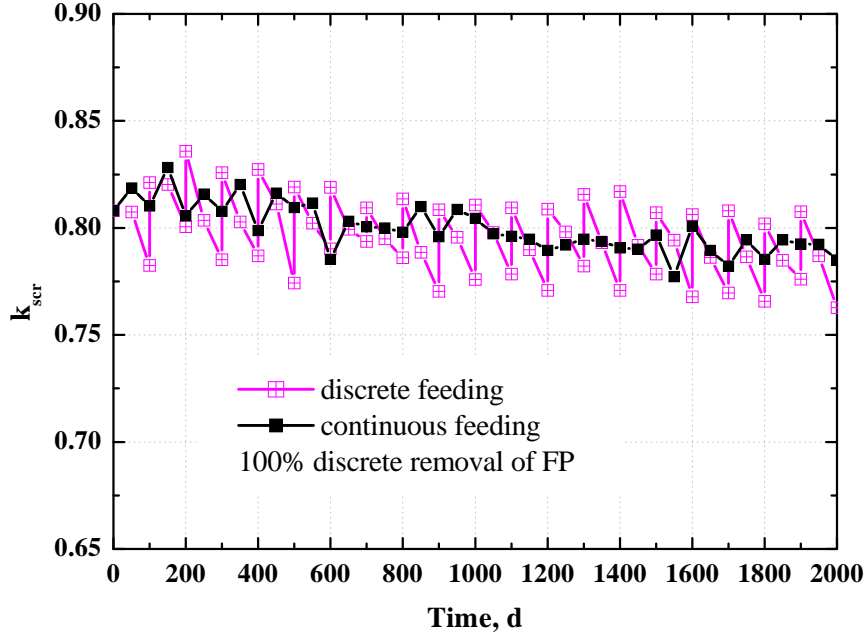


Figure 9:  $k_{scr}$  as a function of discrete and continuous TRU feeding and with discrete removal of all (100%) fission products at the end of steps.

$k_{scr}$  (consequently, possible sharp variations of the reactor power). Of course, this effect could be diminished with additional control rods. On the other hand, the situation is improved considerably if continuous feeding option is chosen (see the same Fig. 9).

We also note separately that in both cases as above a slightly different isotopic composition at equilibrium stage is obtained (see Table 8). As it can be seen from Fig. 10, the difference appears mainly in the first step of burnup calculation, after which the behavior of the curves is rather similar. TRU mass at equilibrium with discrete feeding is  $\sim 2770$  kg and with continuous feeding is  $\sim 3100$  kg. The reason for such a difference is the following: in discrete feeding case a fresh TRU material was added at the beginning of each step (100 days long), while in continuous feeding case – it was replenished during each step. Therefore, in the first case less initial material remains in the molten salt from the very beginning. Smaller equilibrium mass of TRU material could be important for system safety requirements. On the other hand, discrete feeding results in sharp fluctuations of  $k_{scr}$ , as already discussed above, and what would be difficult to tolerate in the realistic system.

One could also ask if different feeding options could change the equilibrium conditions.

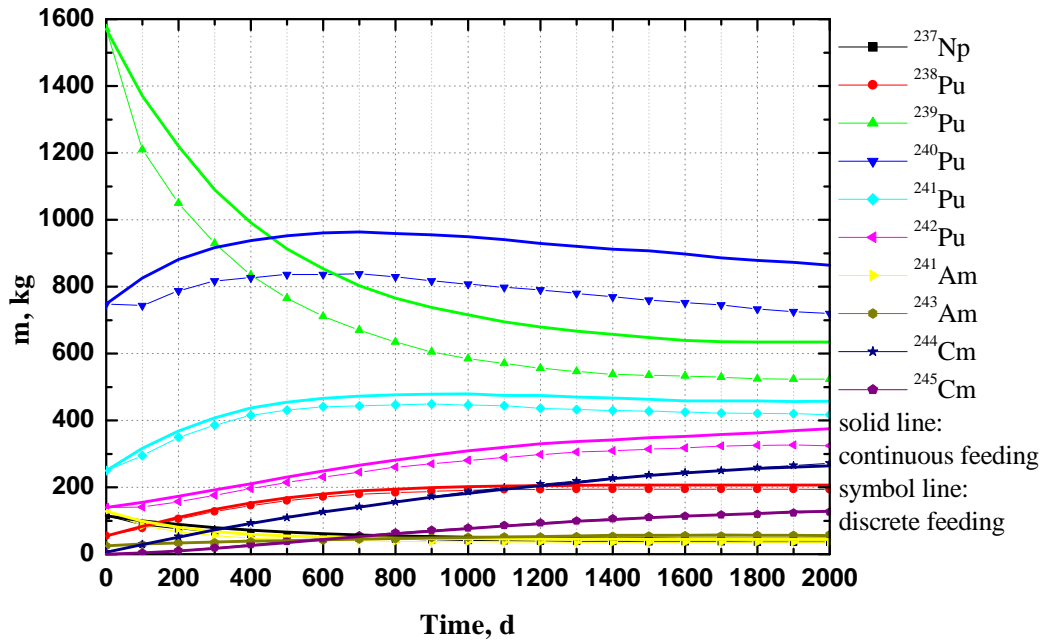


Figure 10: TRU isotopic composition profile in molten salt as a function of irradiation in the cases of discrete and continuous feeding.

Fig. 11 clearly shows that in both cases (with discrete and continuous feeding),  $^{239}\text{Pu}$  mass equilibrates with the same speed. In other words, less than 4% variation is achieved in both cases at the same time. The same is also true for other isotopes of plutonium.

### 3.4 Effect of fission products

The importance of fission products in the molten salt blanket for fusion-fission hybrid system was already analyzed in detail in Ref. [3]. It was concluded that on line removal and disposal of some neutron poisonous fission products may be needed in order to reach deep burnup level and, at the same time, to keep the effective neutron multiplication coefficient of the system (equally blanket fission power) as close to the initial value as possible. In the same study it was found that fission products are responsible at least for  $-3150$  pcm decrease in the effective neutron multiplication coefficient at 15% burnup. It was also pointed out that the tolerance of the fission products in molten salt may allow a batch process, and the allowable burnup tolerance level could be about 10% or slightly more.

Fig. 12 presents the behavior of  $k_{scr}$  when all fission products are removed in two different modes, i.e. continuously and discretely. It seems that the way fission products are removed (as long as they are removed 100%) has little influence on the performance of the system. On the other hand, the percentage of removed FP relative to the total mass of fission products present in the blanket becomes crucial as shown in Fig. 13.

Four different scenarios were considered with the following FP removal options: 100%, 50%, 20% and 0% respectively. 0% corresponds to the case when all fission products are left in the molten salt flibe, while in the case of 100% - all fission products are removed.

In the first case  $k_{scr}$  is rather stable during all the irradiation time. Removing of 50% of fission products has no significant influence on the behavior of  $k_{scr}$ . In this case we conclude that

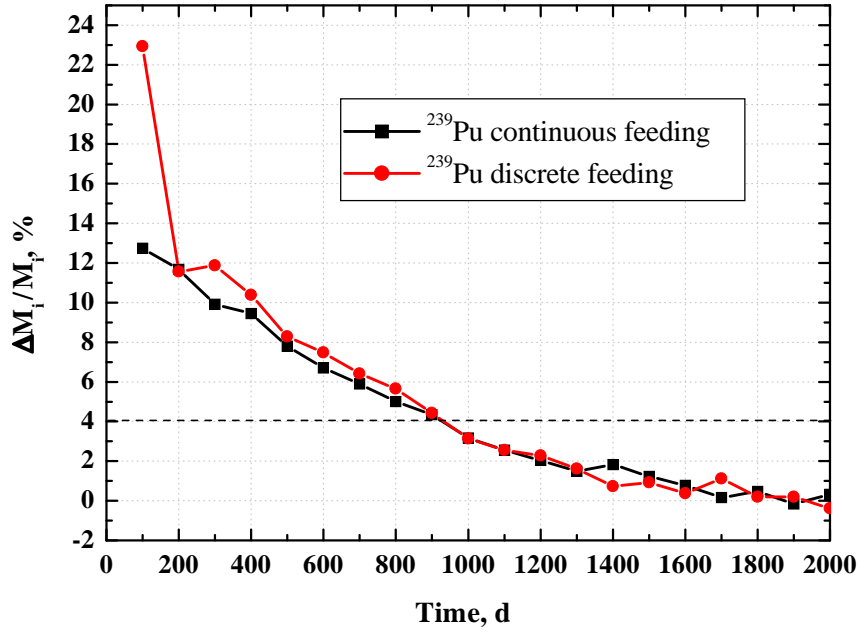


Figure 11: Variation in mass (%) of  $^{239}\text{Pu}$  as a function of the irradiation time in the cases of continuous and discrete feeding and with 100% removal of FP.

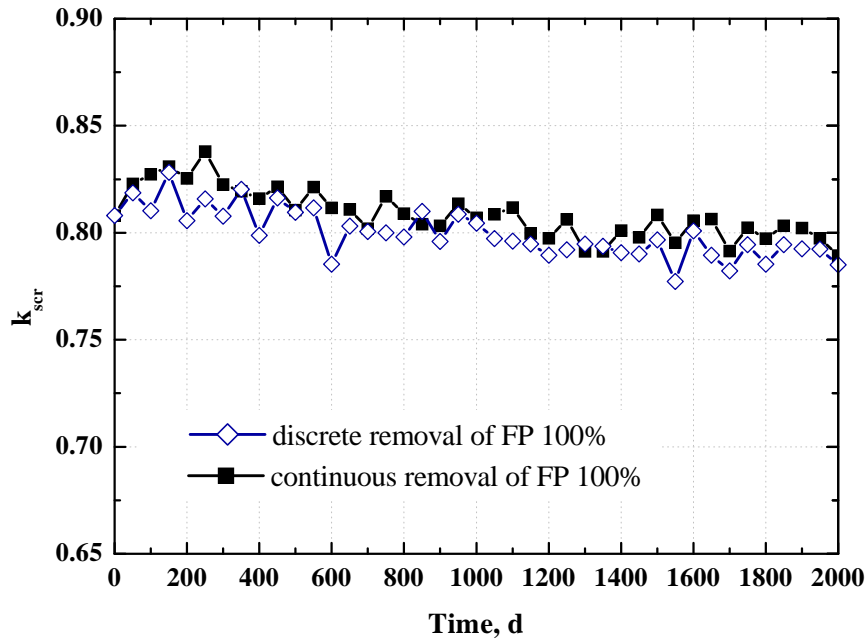


Figure 12: Comparison of  $k_{scr}$  in the case of continuous feeding but different removal of fission products.

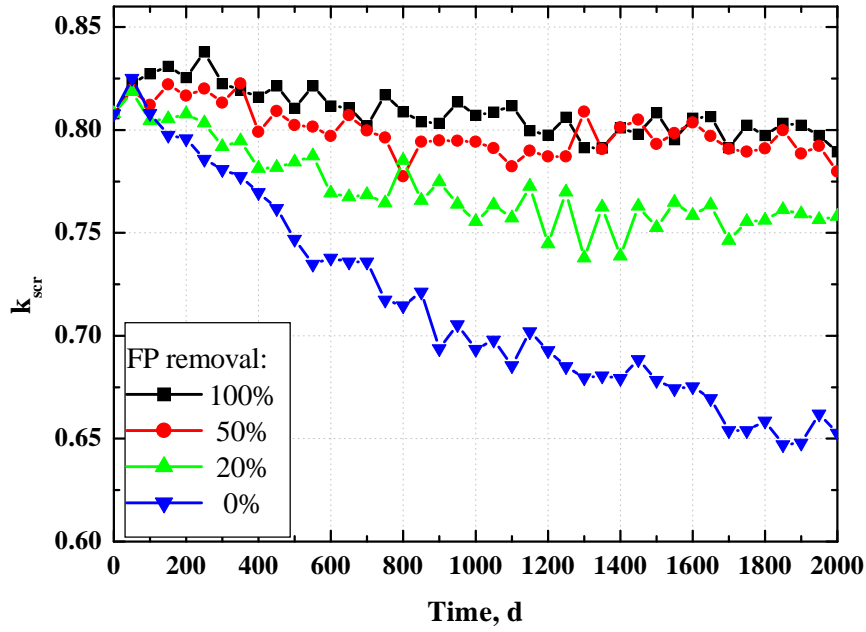


Figure 13:  $k_{scr}$  as a function of different percentage of fission products removed from the fuel.

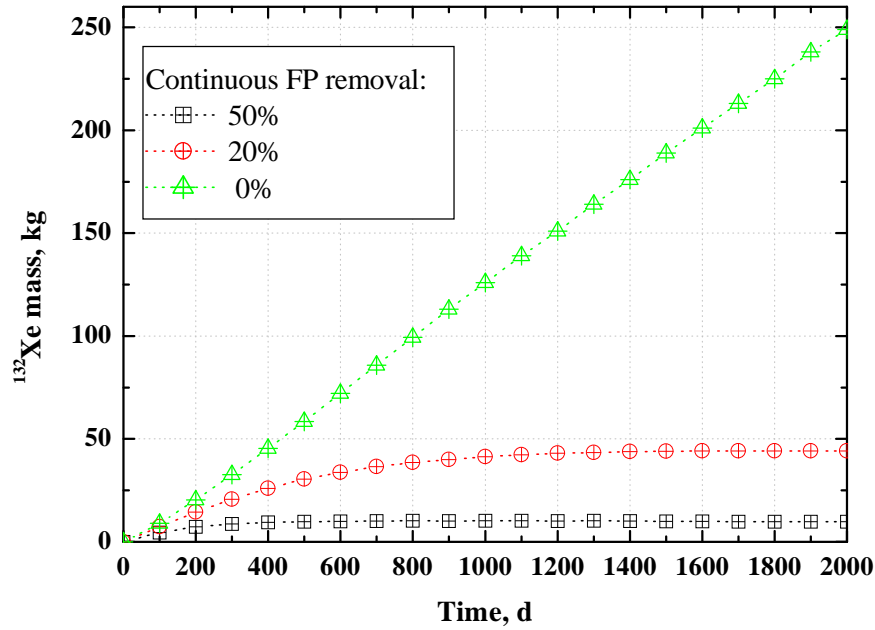


Figure 14: Mass variation of the stable fission product  $^{132}\text{Xe}$  during the irradiation time in the case of continuous feeding of TRU and different removal percentage of fission products.

at least 50% of the fission products have to be taken away from the flibe blanket. When only 20% of fission products are removed, due to the accumulation of fission products,  $k_{scr}$  decreases from 0.81 to 0.76, and from 0.81 to 0.65 when all the fission products are left. This would imply to the corresponding intensity increase of the external neutron source to keep the reactor fission power constant.

One can ask, why there is such a big difference between removal of 50%, 20% and 0% fission products. This can be explained by analyzing the creation/destruction and removal ratios of the fission products. We will take, for example, a stable fission product  $^{132}\text{Xe}$ , which has a small neutron capture cross-section. In Fig. 14 we present its mass as a function of burnup when either all or part of the fission products are left. When all fission products are left, the amount of  $^{132}\text{Xe}$  increases linearly (triangles).

When 20% of FP are taken away, the  $^{132}\text{Xe}$  mass reaches the equilibrium after  $\sim 1200$  days and later its mass remains stable; in the case of 50% removal, the equilibrium is reached already after  $\sim 400$  days. It should be pointed out separately that as long as fission products reach equilibrium,  $k_{scr}$  also varies very little (compare the curves in Fig. 13 keeping in mind the corresponding curves in Fig. 14). Rather similar situation will be with other (stable or long-lived and with similar capture cross sections) fission products – they will reach equilibrium at different times and at different quantities. For the rest of fission products (short lived or with high capture cross sections) the equilibrium may be reached much faster and even without removal.

Finally, we add that a mechanism to remove the fission products is definitely needed in the molten salt based transmutation system. This has to be done not only due to the neutronics of the system as discussed above but also due the following reason. The burn-up of the TRU materials is about 1.1 metric tons per year, equivalent to about 30% TRU inventory in the blanket. Solidification of fission products or TRU materials will occur in the molten salt quite soon after the operation, if some fission products are not removed. The next study of this area would be to look into the strategy and reality how these fission products can be removed.

### 3.5 Conclusions

The performance a fusion-fission hybrid system based on the molten salt (flibe) blanket, driven by a plasma fusion device and dedicated to burn actinides extracted from the LWR spent fuel TRU, was analyzed. Detailed burnup calculations with different modes of replenishing the destroyed TRU material and also with different treatment of fission products were done using Monteburns code system. Major system's performance parameters (e.g.,  $k_{scr}$ ,  $\Phi_n(E)$ , equilibrium conditions, etc.) were investigated. We conclude that

- \* Equilibrium concentration for most of the TRU materials in the blanket can be achieved after about 3 years of exposure. Such a plant could annually burn about 1.1 metric tons of spent fuel actinides. At equilibrium, significant amount of curium isotopes is to be accumulated, while for the rest of actinides fully equilibrated concentrations are reached.

- \* Different replenishing of the destroyed TRU material was tested (continuous and discrete feeding). A stable neutron energy spectrum was obtained in both cases. The behavior of  $k_{scr}$  in the case of a discrete feeding has sharp fluctuations if compared with continuous feeding. On the other hand, different refueling options lead to different TRU mass in the blanket at equilibrium (3100 kg and 2770 kg with continuous and discrete feeding respectively). Although a smaller TRU mass at equilibrium is preferred due to safety reasons, a more stable system's performance obtained in the case of a continuous feeding is recommended.

- \* Accumulation of fission products in the blanket was investigated including their influence

on the performance of the system. We found that  $k_{scr}$  is rather stable during all the irradiation time (0.81-0.79) when all or at least 50% of fission products are taken away. The removal of a smaller percentage of fission products is not recommended since  $k_{scr}$  would fall down considerably (e.g., 0.81→0.76 and 0.81→0.65 with only 20% or 0% FP removal respectively within 2000 days).

Our future studies will concentrate on the detailed performance analysis of the system depending on different data libraries used.

## References

- [1] E.T. Cheng and Clement P.C. Wong, "Transmutation of Actinide in Fusion Reactors and Related Systems Analysis", Proc. of the 10th Int. Conf. on Emerging Nuclear Energy Systems (ICENES'2000), Petten, The Netherlands, September 24-28, 2000; pg. 251.
- [2] E.T. Cheng, "Characteristics of Promising Transmutation Blanket Concepts", Proc. of this International Workshop on Blanket and Fusion Concepts for the Transmutation of Actinides, 21-23 March 2001, General Atomics, San Diego, California, U.S.A.
- [3] D. Ridikas *et al.*, "Importance of Fission Products in the Molten Salt Blanket for Fusion-Fission Hybrid Systems", Proc. of the Int. Workshop on Blanket and Fusion Concepts for the Transmutation of Actinides, 21-23 March 2001, General Atomics, San Diego, California, U.S.A.
- [4] H.R. Trelue and D.I. Poston, "User's Manual, Version 2.0 for Monteburns, Version 5B", LANL, *preprint LA-UR-99-4999* (1999).
- [5] J. Briesmeister for Group X-6, "MCNP-A, A General Monte Carlo Code for Neutron and Photon Transport", Version 4A, LANL, *preprint LA-12625-M* (1993).
- [6] RSIC Computer Code Collection, "ORIGEN 2.1 - Isotope Generation and Depletion Code Matrix Exponential Method", Radiation Shielding Information Center, *report CCC-371* (1991).
- [7] D. Ridikas *et al.*, "On the Fuel Cycle and Neutron Fluxes of the High Flux Reactor at ILL Grenoble", Proc. of the 5th Int. Specialists Meeting SATIF-5, 17-21 July 2000, OECD/NEA Paris, France.
- [8] D. Ridikas *et al.*, "Modelling of Critical and Sub-critical GT-MHRs for Waste Disposal and Proliferation-Resistant Fuel Cycles", Proc. of the 6th OECD/NEA Information Exchange Meeting on Actinide and Fission Product Partitioning and Transmutation, 11-13 December 2000, Madrid, Spain.
- [9] D. Ridikas *et al.*, "Comparative Analysis of the ENDF, JEF and JENDL Data Libraries by Modelling High Temperature Reactors (GT-MHR) and Plutonium Based Fuel Cycles", Proc. the Int. Conference on Nuclear Data for Science and Technology, ND2001, Oct. 7-12, 2001, Tsukuba, Ibaraki, Japan.
- [10] ENDF/B-VI, "The US evaluated neutron nuclear data library for neutron reactions", IAEA-Vienna, IAEA-NDS-100, Rev. **6** (1995).
- [11] JENDL-3.2, "The Japanese Evaluated Nuclear Data Library", IAEA-Vienna, IAEA-NDS-110, Rev. **5** (1994).